

ERROR MOTIONS OF A NON-ORTHOGONAL ROTARY AXIS

Michael L. McGlaufflin¹, Shawn P. Moylan¹

¹Machine Tool Metrology Group
Manufacturing Metrology Division
Manufacturing Engineering Laboratory
National Institute of Standards and Technology
Gaithersburg, Maryland, USA

INTRODUCTION

Error motions of rotary axes are among many sources of imprecision in machining. International and U.S. national standards on machine tool performance contain parameters and procedures to quantify these error motions [1, 2].

The National Institute of Standards and Technology employs a 5-axis machining center that utilizes a "B-axis" which is oriented in the YZ plane at a -45° angle to the Y-axis. This unusual configuration creates a challenge when attempting to measure axis of rotation error motions. A non-orthogonal orientation introduces considerations regarding location, alignment, and coverage area of the measurement artifact as they relate to standoff distances, indicator range, and fixture interference. Subsequent consideration must also be given to the proper analysis of the resultant data to correctly orient the error-motions to the machine coordinate system.

This paper describes a method for determining rotating sensitive direction [1] error-motions of a rotary axis whose axis of rotation is -45° to the X/Y plane. The method is based on a spindle-mounted touch-trigger probe and simple table-mounted spherical artifact. The method was compared to more traditional non-contact measurements (capacitance sensors) to validate the results. The paper also describes the analysis procedures and an evaluation of the measurement uncertainty [3].

DESCRIPTION OF THE TEST MACHINE AND SIGN CONVENTIONS

The machine tool used in this research is a vertical five-axis high-speed machining center with an integrated strain-gage type, touch-trigger probe.

The machine is comprised of stacked slides (Z on Y on X) that move the tool and separately

stacked rotary axes (C on B) that move the work-piece (Figure 1). For purposes of clarity, the manufacturer's nomenclature will be used regarding the B-axis although its axis of rotation is not parallel to the Y-axis. Position feedback is provided by linear and rotary glass scales.

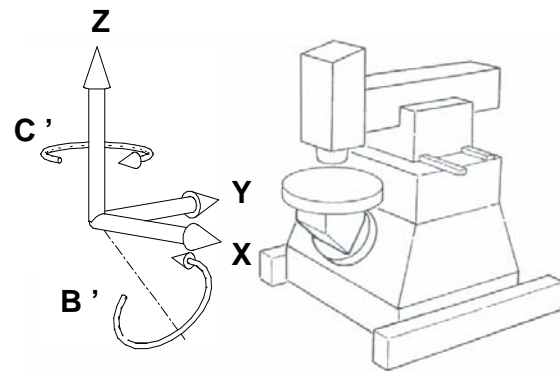


FIGURE 1. Machine-tool structure and sign convention.

MEASUREMENT AND ANALYSIS PROCEDURES

A 25.4 mm, grade 5 gage sphere ($0.13 \mu\text{m}$ sphericity) was mounted on the rotary table in two different measurement locations (Locations I and II) and probed every 5 degrees of the B-axis rotation from 0° to 180° (the maximum travel of the axis) for a total of 37 data sets per run. Location I was aligned to the C-axis of rotation 100 mm below the Point of Rotation (POR), so named because its position in the machining volume does not change as the B-axis rotates. Location II was also aligned to the C-axis 50 mm above the POR. Thirty test runs were performed at each location. Figure 2 illustrates how the sphere center locations vary as the B-axis rotates. With a feedrate of 300 mm/min for probing and a B-axis positioning feedrate of $1575^\circ/\text{min}$ (10 % of rapid rate), the total time per test was five hours.

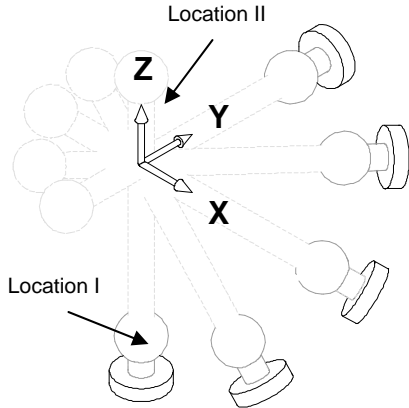


FIGURE 2. Artifact orientation as B-axis rotates

The position of the center of the spherical artifact at each B-axis position was determined by probing nine points on the surface using vector-normal probing and least squares fitting. The locations obtained by probing, and thus the center location estimated by the sphere fitting algorithm, are in the machine coordinate frame. To align them in a plane perpendicular to the B-axis, the center positions are multiplied by a coordinate transformation matrix, a simple -45° rotation around the machine's X-axis.

Following procedures outlined in the standards, a least-squares circle is fit to the 37 sphere center positions [1, 2]. The distances from the sphere center locations to the best-fit circle represent the radial error-motion of the B-axis. The probing and analysis procedure is repeated for thirty data sets, allowing synchronous and asynchronous error motion to be determined. Figures 3 and 4 show the radial error motion. Figure 5 shows the synchronous radial error-motion at sphere locations I and II.

The synchronous tilt error motion is the difference in the synchronous error motion components divided by the distance between them ($150 \text{ mm} * \cos 45^\circ$) at each B-axis position (Figure 6). The asynchronous tilt error motion value at Locations I and II was $17.9 \mu\text{rad}$. It is important to note that the asynchronous value stated here was calculated from data gathered sequentially. While the data was collected at the same nominal positions of the B-axis, the actual positions vary.

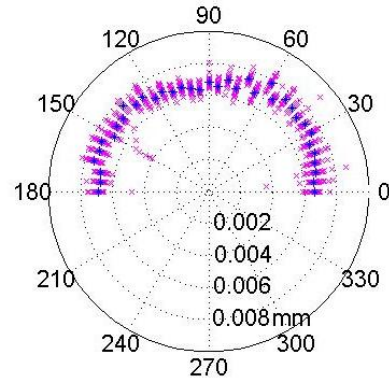


FIGURE 3. Radial error motion at Location I Asynchronous error motion ($4.2 \mu\text{m}$)

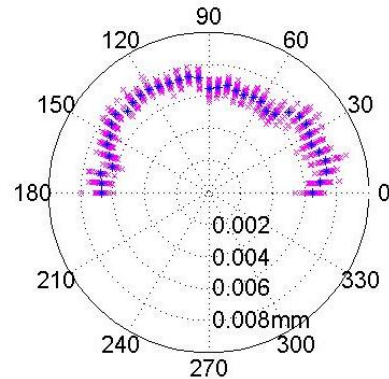


FIGURE 4. Radial error motion at Location II Asynchronous error motion ($2.3 \mu\text{m}$)

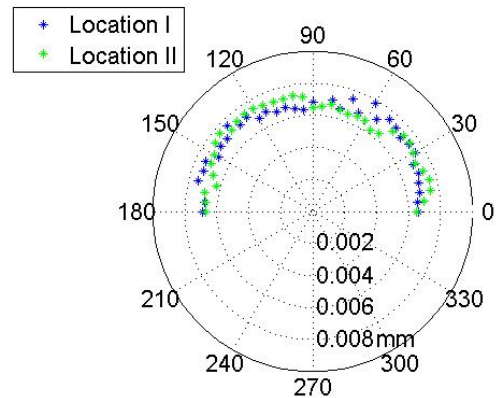


FIGURE 5. Synchronous radial error motions; Location I ($1.4 \mu\text{m}$) Location II ($1.4 \mu\text{m}$).

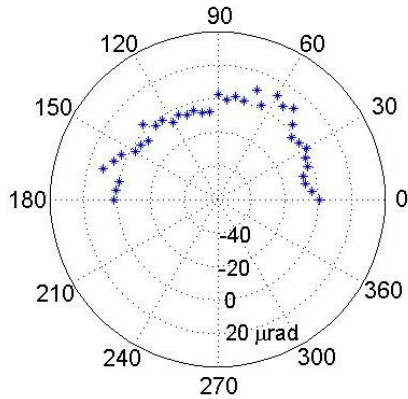


FIGURE 6. Synchronous tilt error motion value (17.9 μrad)

Face error motion at Location I was calculated using the Z component of the sphere center points after the coordinate transformation. Figure 7 shows the synchronous face error motion. Asynchronous face error motion was 6.7 μm .

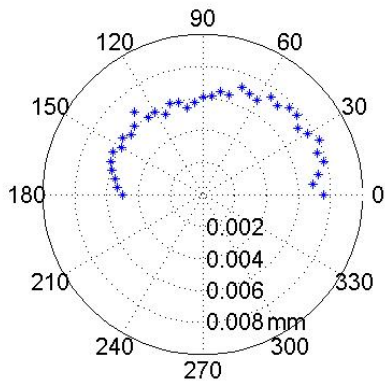


FIGURE 7. Synchronous face error motion at Location I (3.1 μm)

VERIFICATION TESTS AND RESULTS

Verification tests were executed by conducting probing and capacitance sensor tests on the C-axis of the machining center. The C-axis is oriented parallel to the machine's Z-axis, making axis of rotation testing more straightforward and therefore more suitable for verification. Probing data was taken every 10° as the axis rotated through 360° for a total of 37 data points.

Capacitance sensor data were gathered as the axis continuously rotated through 360° at a speed of 1575 °/min . To maintain the rotating sensitive direction orientation, the spherical

artifact was fixtured in the machine spindle, which remained stationary, and a capacitance sensor was attached to the work table in a radial direction and rotated with the C-axis. The sensor was oriented in the negative X direction (when C = 0).

Analysis of both probing and capacitance sensor data was similar to the analysis of the B-axis data. However, because the C-axis is an orthogonal axis, the coordinate transformation is not necessary. A least squares circle fit was applied to the raw capacitance sensor data, and the deviation from the best fit circle was calculated.

Figure 8 shows a comparison of the measurement results for synchronous radial error motion determined by the two methods.

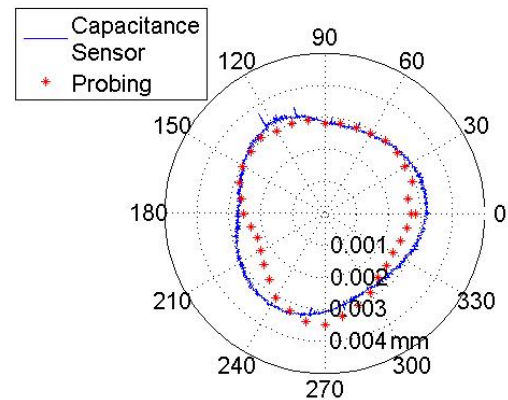


FIGURE 8. Synchronous radial error-motion of the C-axis; capacitance sensor vs. probing. Synchronous error value probing (1.2 μm); capacitance sensor (1.1 μm); asynchronous error value probing (1.6 μm); capacitance sensor (1.0 μm).

UNCERTAINTY ANALYSIS

The main contributors to the uncertainty of measurements by probing are probing repeatability, positioning accuracy of the linear axes, and thermal growth.

The machine has a well documented thermal behavior due to machine startup sources such as electrical and mechanical systems and lubrication. To minimize this influence, a simple procedure was followed at the beginning of each day's data collection. The machine was initialized, homed, left to stabilize for a minimum of 2 hours, and then run through a short 5-axis

lubrication program to ensure the axes were properly lubricated.

Because the linear axes are moving during probing and stationary during capacitance sensor tests, the influence of motion-induced thermal growth and the large amount of time required to collect probing data as compared to that required for capacitance data are the largest sources of uncertainty in the comparison. The value for this uncertainty came from previously compiled data of the entire work volume. Since the probing occurred in a small portion of the volume, we estimated the drift corresponding to that portion as $X = 1 \mu\text{m}$, $Y = 13 \mu\text{m}$, and $Z = 3 \mu\text{m}$.

For the purposes of this discussion, probing repeatability for 3 dimensional probing systems is the ability of the machine/probe system to locate the center of a stationary spherical artifact by touching the surface of the sphere at multiple locations. We determined this error by repeatedly probing a spherical artifact at nine uniformly distributed points. Thirty measurement cycles were performed with no rotation of the rotary axes and no interruption between cycles. A least squares spherical fit was applied to each data set and the standard deviation of the 30 center X, Y, and Z positions calculated. Probe lobing was included in this determination.

The location of the target sphere changes as the B-axis rotates. Therefore the geometric errors of the machine can result in uncertainty in probing data due to the volumetric accuracy of the machine. However, as explained previously, the probing head moves through a small portion of the work volume so this contribution to the combined standard uncertainty is small ($0.3 \mu\text{m}$).

Thermal growth of the artifact was not significant due to the minimal contribution from the sphere and the invar material for the support column for the sphere.

The combined standard uncertainty estimation is given in Table 1.

TABLE 1. Estimated uncertainty for the probing method.

Source	Std.Uncertainty (μm)
Thermal Growth	13.4
Probing Repeatability	0.5
Volumetric Accuracy	0.3
Combined Std. Uncertainty	13.4
Expanded Uncertainty ($k=2$)	26.8

CONCLUSIONS

Probing appears to be a viable option for characterizing axis of rotation error motions of non-orthogonal rotary axes. The comparison data in Figure 8 show a good correlation in form and magnitude. The uncertainty related to thermal growth overshadows the surprisingly small uncertainties related to probing error and volumetric accuracy.

The test is easy to set up and align, and doesn't require expensive equipment. The extreme difficulty in aligning an artifact to a non-orthogonal axis of rotation makes traditional methods of eliminating artifact alignment error prohibitively complicated and time consuming.

A thorough understanding of the sources of uncertainty could allow probing to provide a cost- and time-effective alternative to traditional axis of rotation measurements of complicated machine designs. The uncertainty related to thermal growth could be reduced by a modified warm-up procedure. Previous thermal expansion tests [4] indicate a three hour 5-axis motion period prior to testing could potentially reduce this uncertainty to less than $8 \mu\text{m}$.

REFERENCES

- [1] ISO 230-7, Geometric Accuracy of axes of rotation.
- [2] ANSI/ASME B89.3.4M, Axes of Rotation Methods for Specifying and Testing, 1985.
- [3] NIST TN1297, Guidelines for Evaluating and Expressing the Uncertainty of NIST Measurement Results, 1994.
- [4] ISO 230-3, Test code for machine tools— Part 3: Determination of thermal effects, 2001.

This Publication was prepared by a United States Government employee as part of official duties and is, therefore, a work of the U.S. Government and not subject to copyright.